Speckle Propagation through Atmospheric Turbulence: Effects of a Random Phase Screen at the Source

O. Korotkova*[a], L. C. Andrews**[a], R. L. Phillips***[b]
[a]Dept. of Mathematics, Univ. of Central Florida; [b]Florida Space Institute

ABSTRACT

By using *ABCD* ray matrix theory and a random phase screen located near the source, analytic expressions are developed for the mutual coherence function and scintillation index of a Gaussian-beam wave propagating through weak atmospheric turbulence in both the pupil plane and image plane of a receiving system. The phase screen model that we use is based on a previous double-pass analysis by the authors for analyzing speckle propagation from a rough target in a lidar system. In the present context, it serves as a model for a partially coherent Gaussian-beam wave that is currently used in laser communications. The effect of partial coherence (induced by a diffuser) on the scintillation index of the beam in the presence of weak atmospheric turbulence is investigated as a function of the correlation length of the diffuser and the propagation distance.

1. INTRODUCTION

The fundamental results on the propagation of partially coherent beam in the atmospheric turbulence were established in late 1970s and early 1980s. However, an increasing interest in this area currently occurs due to its potential application in laser communications, where partial coherence might be used to defeat scintillation index (and, consequently, bit-error rates).

The first indication that the spatial partial coherence of the source reduces scintillation can be found in [1]. The mutual coherence function (MCF) of the quasi-monochromatic partially coherent source with Gaussian profile is formulated in [2,3]. In recent work [4], Gaussian beam characteristics (average intensity, beam size, phase front radius of curvature, wavefront coherence length) were derived from the cross spectral density (the counterpart of the MCF in the frequency domain). The analysis of coherence radius of spatially partially coherent beam belongs to [5]. Conventionally partial coherence of the beam is modeled by placing the diffuser in the transmitter aperture (described by a Gaussian Schell-model [6]).

The analytic expressions for the intensity correlation function in weak and strong turbulence for a spatially partially coherent beam were formulated in [7] using the extended Huygens-Fresnel principle, and in [8] using the extended Rayleigh-Sommerfeld solution. In [9], the Rytov method was used to approximate it in the weak atmospheric regime. Scintillation due to a temporally partially coherent wave was derived in [10]. The discussion about the difference between the scintillation index in the systems with slow and fast detection belongs to [7]. The effect of spatial partial coherence on the bit error rates was investigated in [4].

Classic methods commonly used in the literature (such as extended Huygen-Fresnel integral) did not lead to tractable expressions, even for second-order statistics involving actual atmospheric spectrums (a Gaussian approximation was used, for example, in [4]).

Our approach to this problem is based on a model established in earlier work [11] for a rough target in a laser radar scenario involving a complex phase screen model for the target together with Rytov theory and ABCD ray matrices. In this paper we extend that analysis to the single-pass lasercom link and give all statistics for the free space propagation as well as for atmospheric turbulence. Our expressions are based on the Kolmogorov spectrum, but in fact, they can be easily reproduced for any other spectrum model including inner and outer scale.

2. MODEL

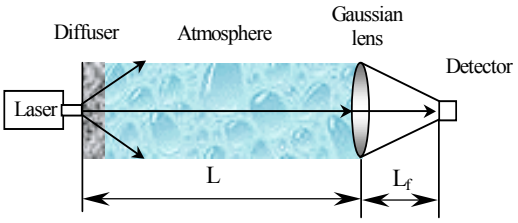

Figure 1. Propagation of partially coherent beam

A schematic diagram for the propagation of a partially coherent beam is shown in Figure 1. We assume the transmitted beam wave is a TEM_{00} Gaussian-beam wave characterized by parameters

$$\Theta_0 = 1 - \frac{L}{F_0}, \qquad \Lambda_0 = \frac{2L}{kW_0^2}, \tag{1}$$

where k (m^{-1}) is the laser wave number, L (m) is propagation distance to the collecting lens, F_0 (m) is the phase front radius of curvature, and W_0 (m) is the laser exit aperture radius. We model the boundary layer (diffuser) as a Gaussian thin phase screen with spectrum model [11]

$$\Phi_s(\kappa) = \frac{\langle n_1^2 \rangle l_c^3}{8\pi\sqrt{\pi}} exp\left(-\frac{1}{4} l_c^2 \kappa^2\right) \tag{2}$$

where κ (m^{-1}) is the atmospheric wave number, l_c (m) is the lateral correlation radius directly related to the variance σ_g^2 of the Gaussian phase screen used in [4] by

$$l_c^2 = 2\sigma_g^2, \tag{3}$$

and $\langle n_1^2 \rangle$ is the fluctuation in the index of refraction induced by the screen.

Although the diffuser does not initially change the size of the beam, the scattering effect associated with scintillation of a partially coherent beam can be modeled by introducing an "effective" radius of curvature

$$\frac{1}{F_{after\_screen}} = \frac{1}{F_0} + \frac{1}{F_R}, \tag{4}$$

where F_R is the phase front radius of curvature induced by the diffuser. This quantity must be a function of the strength of the screen but its functional form is not known at this time. We introduce nondimentional quantity q_c by

$$q_c = \frac{L}{kl_c^2}, \tag{5}$$

relating the strength of the screen to first Fresnel zone. The focusing effect of this model describes only a portion of the whole actual beam, which is related to the amount of scattering. To distinguish between them we call our beam and its characteristics (for the scintillation index) "effective." Although for second-order statistics the effective part of the beam does not carry physical meaning, we will show that the result for the scintillation index does reproduce the actual trend, which will be discussed in Section 3.1. Following [12], we introduce parameters Λ_1, Θ_1 for the beam incident on the collecting lens (of radius W_1 and phase front radius of curvature F_1):

$$\Lambda_1 = \frac{\Lambda_0}{\Theta_0^2 + \Lambda_0^2}, \qquad \Theta_1 = \frac{\Theta_0}{\Theta_0^2 + \Lambda_0^2} \tag{6}$$

After passing through the Gaussian lens at the receiver of radius W_G and phase front radius of curvature F_G, and propagating to the detector plane at distance L_f from the lens, the beam of radius W_2 and radius of curvature F_2 is characterized by

$$\Lambda_2 = \frac{L}{L_f}\left[\frac{\Lambda_1 + \Omega_G}{\left(\frac{L}{L_f} - \frac{L}{F_G} + \overline{\Theta}_1\right)^2 + (\Lambda_1 + \Omega_G)^2}\right], \qquad \Theta_2 = \frac{L}{L_f}\left[\frac{\frac{L}{L_f} - \frac{L}{F_G} + \overline{\Theta}_1}{\left(\frac{L}{L_f} - \frac{L}{F_G} + \overline{\Theta}_1\right)^2 + (\Lambda_1 + \Omega_G)^2}\right], \tag{7}$$

where $\overline{\Theta}_1 = 1 - \Theta_1$ and the nondimensional parameter Ω_G is defined by

$$\Omega_G = \frac{2L}{kW_G^2}. \tag{8}$$

In the image plane of the system $\Theta_2 = 0$.

The ABCD ray matrix for the pupil plane of the optical system is

$$\begin{pmatrix} A & B \\ C & D \end{pmatrix} = \begin{pmatrix} 1 & L \\ 0 & 1 \end{pmatrix}, \tag{9}$$

while for the image plane of the receiver it takes the form

$$\begin{pmatrix} A & B \\ C & D \end{pmatrix} = \begin{pmatrix} 1 & L_f \\ 0 & 1 \end{pmatrix} \begin{pmatrix} 1 & 0 \\ i\alpha_G & 1 \end{pmatrix} \begin{pmatrix} 1 & L \\ 0 & 1 \end{pmatrix} = \begin{pmatrix} 1+i\alpha_G L & L+L(1+i\alpha_G L) \\ i\alpha_G & 1+i\alpha_G L \end{pmatrix} \tag{10}$$

where $\alpha_G = \frac{2}{kW_G^2} + i\frac{1}{F_G}$.

Comparing the model under study with the model introduced in [11] we find that sets of parameters defined by (1), (6) and (7) are the same as sets $\Lambda_1 + \Omega_R$, Θ_1; Λ_2, Θ_2 and Λ_3, Θ_3 respectively defined for the laser radar system. Parameter Ω_R in [11] that takes into account the finite size of the target now is absorbed by transmitted beam parameter Λ_1. Therefore all results of the previous work can be reproduced for the partially coherent system by simple shift of parameters.

3. FREE SPACE PROPAGATION.

3.1 Pupil plane.

In the plane of the collecting lens the mutual coherence function (MCF) of the Gaussian beam is [12]

$$\begin{aligned} \Gamma_d(\mathbf{r}_1, \mathbf{r}_2, L) &= \Gamma_0(\mathbf{r}_1, \mathbf{r}_2, L) exp\left\{ -4\pi^2 k^2 \Delta z \int_0^\infty \kappa \Phi_s(\kappa) \left(1 - e^{\Lambda_1 L \kappa^2 / k} \right) J_0\left(\kappa \left| \Theta_1 \mathbf{p} - 2i\Lambda_1 \mathbf{r} \right| \right) d\kappa \right\} = \\ &= \Gamma_0(\mathbf{r}_1, \mathbf{r}_2, L) exp\left[\sigma_d^2(\mathbf{r}_1, L) + \sigma_d^2(\mathbf{r}_2, L) \right] exp\left[-T_d \right] exp\left[-\frac{1}{2} \Delta_d(\mathbf{r}_1, \mathbf{r}_2, L) \right] \end{aligned} \tag{11}$$

where $\Gamma_0(\mathbf{r}_1, \mathbf{r}_2, L)$ is the mutual coherence function in absence of the phase screen defined by

$$\Gamma_0(\mathbf{r}_1, \mathbf{r}_2, L) = \frac{W_0^2}{W_1^2} exp\left(-\frac{2r^2}{W_1^2} - \frac{\rho^2}{2W_1^2} - i\frac{k}{F_1} \mathbf{p} \cdot \mathbf{r} \right) \tag{12}$$

and $\mathbf{r} = \frac{1}{2}(\mathbf{r}_1 + \mathbf{r}_2)$, $\boldsymbol{\rho} = \mathbf{r}_1 - \mathbf{r}_2$, $r = |\mathbf{r}|$, $\rho = |\boldsymbol{\rho}|$. In (11) all exponential terms are perturbations due to the screen. They are based on the ray matrix (9). Appling the Gaussian spectrum (5) for the phase screen, the radial component of MCF, $\sigma_d^2(\mathbf{r}, L)$, is easily derived

$$\sigma_d^2(r, L) = \frac{\sqrt{\pi} k^2 L \langle n_1 \rangle^2 l_c d_2}{2(1 + 4\Lambda_1 q_c)} \left[exp\left(\frac{4\Lambda_1^2 r^2}{l_c^2 (1 + 4\Lambda_1 q_c)} \right) - 1 \right], \tag{13}$$

where $d_2 = \frac{\Delta z}{L}$, and Δz is the thickness of the screen. After the normalization

$$\frac{\sqrt{\pi} k^2 L \langle n_1 \rangle^2 l_c d_2}{(1 + 4\Lambda_1 q_c)} = 1 \tag{14}$$

and small argument approximation it simplifies to

$$\sigma_d^2(r, L) = \frac{2\Lambda_1^2 r^2}{l_c^2 (1 + 4\Lambda_1 q_c)}. \tag{15}$$

The longitudinal component T_d after normalization (14) and small argument approximation takes the form

$$T_d = 4\Lambda_1 q_c \tag{16}$$

The structure function $Re[\Delta_d(\rho, L)]$ was derived in [3], which in terms of the present parameters yields

$$Re[\Delta_d(\rho, L)] = 2\left(\frac{\Theta_1^2 + \Lambda_1^2}{1 + 4\Lambda_1 q_c}\right)\frac{\rho^2}{l_c^2}. \tag{17}$$

The combination of (11), (15) - (17) gives the following form for the MCF

$$\Gamma_d(\mathbf{r}_1, \mathbf{r}_2, L) = \left(\frac{\Theta_1^2 + \Lambda_1^2}{1 + 4\Lambda_1 q_c}\right) exp\left[-\frac{(2r^2 + \rho^2/2)}{W_1^2(1 + 4\Lambda_1 q_c)}\right] exp\left[-\left(\frac{\Theta_1^2 + \Lambda_1^2}{1 + 4\Lambda_1 q_c}\right)\frac{\rho^2}{l_c^2}\right] exp\left[\frac{ik}{L}\left(\frac{1 - \Theta_1 + 4\Lambda_1 q_c}{1 + 4\Lambda_1 q_c}\right)\mathbf{r} \bullet \mathbf{p}\right]. \tag{18}$$

where we have used the small argument approximation,

$$e^{-T} = \frac{1}{1 + T}. \tag{19}$$

Consequently, the effective beam size due to the phase screen deduced from (18) is

$$W_{1,d} \cong W_1(1 + T)^{1/2} = W_1(1 + 4\Lambda_1 q_c)^{1/2} \tag{20}$$

Expressions (18) and (20) are the same in the form as in [2].

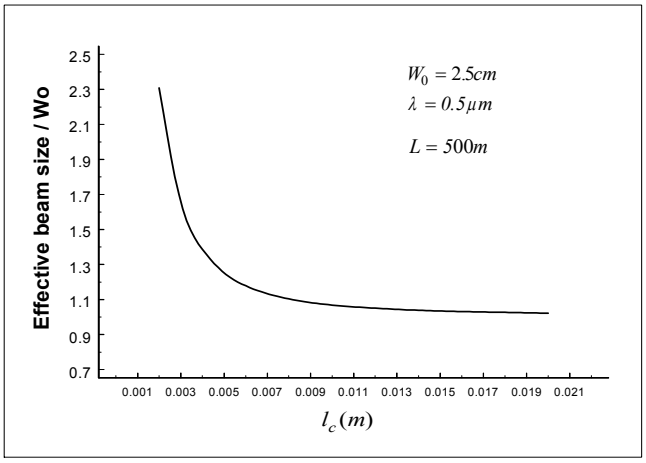

Figure 2. Effective beam size due to diffuser (free space.)

Figure 2 shows the effective beam radius due to the diffuser $W_{1,d}$ scaled by the initial beam radius $W_0 = 2.5cm$ versus the correlation length l_c. Wavelength $\lambda = 0.5\mu m$ The curve represents both the result in [4] and $W_{1,d}$.

The mean irradiance is also easily deduced from (18) taking $\mathbf{r}_1 = \mathbf{r}_2 = \mathbf{r}$ and using approximation (19):

$$\left\langle I_{1,d}(r, L)\right\rangle \cong \frac{W_0^2}{W_1^2} exp\left(-\frac{2r^2}{W_1^2}\right) exp\left(2\sigma_d^2(r, L)\right) exp\left(-T_d\right) = \frac{W_0^2}{W_{1,d}^2} exp\left(-\frac{2r^2}{W_{1,d}^2}\right). \tag{21}$$

Expression (21) agrees in form with [4] as well.

Using our result [11] for the average speckle size in the pupil plane we adapt it for the partially coherent beam by proper shift of propagation parameters:

$$\rho_{1,d} = \sqrt{\frac{(1 + 4\Lambda_1 q_c) l_c^2}{\Lambda_1^2 + \Theta_1^2}}. \tag{22}$$

With help of (20) the speckle size can be rewritten as

$$\rho_{1,d} = \frac{W_{1,d}}{W_0} l_c \,. \tag{23}$$

This simple relation shows that the speckle size in the pupil plane is inversely proportional to the strength of the phase screen and the transmitted power. In the case of a strong diffuser ($l_c \to 0$), Eq. (22) reduces to

$$\rho_{1,d} = \frac{\sqrt{2}\, L\lambda}{\pi W_0} \tag{24}$$

The variance of the angle of arrival fluctuations (under the geometrical optics approximation) [12] depends on the structure function (17) and associated hard aperture diameter of the collecting lens $D_G = 8\,W_G$:

$$\sigma^2_{\beta,d,} = \frac{\Lambda_d\left(D_G, L\right)}{\left(kD_G\right)^2} = \frac{\lambda}{\pi l_c^2}\left(\frac{\Theta_1^2 + \Lambda_1^2}{1 + 4\,\Lambda_1 q_c}\right) = \frac{\lambda W_0^2}{\pi l_c W_{1,d}^2} \tag{25}$$

The next statistic that we calculate is the scintillation index $\sigma^2_{I,d}\left(\mathbf{r}, L\right)$ imposed by the diffuser. For free space propagation the case of fast detector only is considered. In this case the correlation time of the source $\tau_s \cong \frac{1}{B}$, where B is the bandwidth of the source, is much greater than the detector's integration time interval τ_d, i.e. $\tau_s >> \tau_d$ (In the case of a slow detector $\tau_s << \tau_d$ the scintillation index is negligible independently of l_c [3]).

Following the derivation of $\sigma^2_{I,d}\left(\mathbf{r}, L\right)$ in [12] with spectrum model (2), and the same approximations and normalization as described above, the on-axis component of the scintillation index at the collecting lens is

$$\sigma^2_{I,d}\left(0, L\right) = 1 - \frac{\frac{l_c^4}{16}\left(1 + 4\,\Lambda_1 q_c\right)^2}{\frac{l_c^4}{16}\left(1 + 4\,\Lambda_1 q_c\right)^2 + \left(\frac{L\Theta_1}{k}\right)^2} = \frac{\left(\frac{L\Theta_1}{k}\right)^2}{\frac{l_c^4}{16}\frac{W_{1,d}}{W_1} + \left(\frac{L\Theta_1}{k}\right)^2} \tag{26}$$

The functional form of $\sigma^2_{I,d}\left(0, L\right)$ shows that in the case of a weak diffuser the scintillation index approaches zero, whereas for a diffuser with a correlation length on the order of the first Fresnel zone it grows to unity as predicted in [2].

In Figure 3 the effective scintillation index (26) is presented as a function of the correlation length (solid curve). The scintillation index given in [2] is plotted as well (dotted curve).

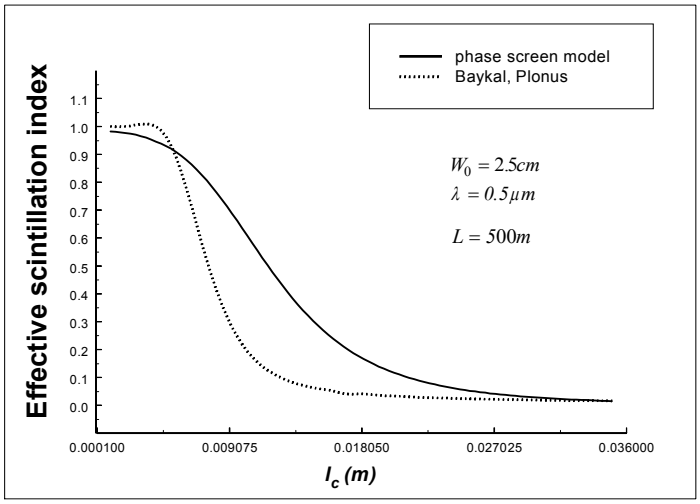

Figure 3. Effective scintillation index vs. correlation length l_c.

3.2 Free space propagation. Image plane.

In the plane of the photodetector the modulus of mutual coherence function due to the phase screen at points $\mathbf{r}_1$ and $\mathbf{r}_2$ is based on the ray matrix (10) and takes the form

$$\left|\Gamma_d\left(\mathbf{r}_1,\mathbf{r}_2,L+L_f\right)\right|=\Gamma_0\left(\mathbf{r}_1,\mathbf{r}_2,L+L_f\right)exp\left[\sigma_d^2\left(\mathbf{r}_1,L+L_f\right)+\sigma_d^2\left(\mathbf{r}_2,L+L_f\right)\right]exp\left[-T_d\right]exp\left[-\frac{1}{2}\Delta_d\left(\mathbf{r}_1,\mathbf{r}_2,L+L_f\right)\right] \quad (27)$$

where the first term is given by

$$\Gamma_0\left(\mathbf{r}_1,\mathbf{r}_2,L+L_f\right)=\frac{W_0^2}{W_2^2}exp\left(\frac{2r^2}{W_2^2}-\frac{\rho^2}{2W_2^2}-i\frac{k}{F_2}\mathbf{p}\cdot\mathbf{r}\right) \quad (28)$$

Based on spectrum (5) the radial component becomes

$$\begin{aligned}\sigma_d^2\left(r,L+L_f\right)=&\frac{1}{2}\sqrt{\pi}\,k^2Ld_2\left\langle n_1^2\right\rangle l_c\frac{\Lambda_1+\Omega_G}{\Lambda_1+\Omega_G+4q_c\left(\Theta_1^2+\Lambda_1\Omega_G\right)}\times\\ \times&\left\{exp\left[\frac{4L^2\Theta_1^2r^2}{L_f^2\left(\Lambda_1+\Omega_G\right)l_c^2\left[\Lambda_1+\Omega_G+4q_c\left(\Theta_1^2+\Lambda_1\Omega_G\right)\right]}\right]-1\right\}\end{aligned} \quad (29)$$

The normalization of (29) is

$$\sqrt{\pi}\,k^2Ld_2\left\langle n_1^2\right\rangle l_c\frac{\Lambda_1+\Omega_G}{\Lambda_1+\Omega_G+4q_c\left(\Theta_1^2+\Lambda_1\Omega_G\right)}=1, \quad (30)$$

and by small argument approximation it simplifies to

$$\sigma_d^2\left(r,L+L_f\right)\cong\frac{2L^2\Theta_1^2r^2}{L_f^2l_c^2\left(\Lambda_1+\Omega_G\right)\left[\Lambda_1+\Omega_G+4q_c\left(\Theta_1^2+\Lambda_1\Omega_G\right)\right]} \quad (31)$$

The longitudinal component of MCF (27) after normalization (30) and small argument approximation is

$$T_d=4q_c\left(\frac{\Theta_1^2+\Lambda_1\Omega_G}{\Lambda_1+\Omega_G}\right) \quad (32)$$

Following [11] the real part of structure function in the image plane can be approximated by

$$Re\left[\Delta_d\left(r_1,r_2,L+L_f\right)\right]\cong\frac{2L^2\left(\Lambda_1^2+\Theta_1^2\right)\rho^2}{L_f^2l_c^2\left(\Lambda_1+\Omega_G\right)\left[\Lambda_1+\Omega_G+4\left(\Theta_1^2+\Lambda_1\Omega_G\right)q_c\right]} \quad (33)$$

Equations (31) – (33) together with (27) give the following result for the modulus of MCF:

$$\begin{aligned}\left|\Gamma_d\left(\mathbf{r}_1,\mathbf{r}_2,L+L_f\right)\right|=&\Gamma_0\left(\mathbf{r}_1,\mathbf{r}_2,L+L_f\right)exp\left[\frac{2L^2\Theta_1^2\left(r_1^2+r_2^2\right)}{L_f^2\left(\Lambda_1+\Omega_G\right)l_c^2\left[\Lambda_1+\Omega_1+4q_c\left(\Theta_1^2+\Lambda_1\Omega_G\right)\right]}\right]\times\\ \times&exp\left[-4q_c\left(\frac{\Theta_1^2+\Lambda_1\Omega_G}{\Lambda_1+\Omega_G}\right)\right]\times exp\left[-\frac{L^2\left(\Theta_1^2+\Lambda_1^2\right)\rho^2}{L_f^2l_c^2\left(\Lambda_1+\Omega_G\right)\left[\Lambda_1+\Omega_G+4q_c\left(\Theta_1^2+\Lambda_1\Omega_G\right)\right]}\right]\end{aligned} \quad (34)$$

Similarly to the case of the pupil plane the beam size and the average speckle size are easily deduced from (34):

$$W_{2,d} = W_2\left(1 + 4\,q_c\,\frac{\Theta_1^2 + \Lambda_1\Omega_G}{\Lambda_1 + \Omega_G}\right)^{1/2}, \tag{35}$$

$$\rho_{2,d} = \sqrt{\frac{L_f^2 l_c^2\left(\Lambda_1 + \Omega_G\right)\left[\Lambda_1 + \Omega_G + 4\,q_c\left(\Theta_1^2 + \Lambda_1\Omega_G\right)\right]}{L^2\left(\Theta_1^2 + \Lambda_1^2\right)}} \tag{36}$$

The concentration factor CF for the Gaussian lens in the detector plane is

$$CF = \left(\frac{\pi W_G^2}{\lambda F_G}\right)^2 \tag{37}$$

Therefore the mean irradiance can be deduced from (21) and (37)

$$\left\langle I_d\left(r, L + L_f\right)\right\rangle = CF \cdot \left\langle I_d\left(r, L\right)\right\rangle = \left(\frac{\pi W_G^2}{\lambda F_G}\right)^2 \frac{W_0^2}{W_{1,d}^2}\,exp\left(-\frac{2\,r^2}{W_{1,d}^2}\right) \tag{38}$$

4. ATMOSPHERIC EFFECTS. PUPIL PLANE.

4.1 Second order statistics.

Because the MCF is primarily due to phase fluctuations, we assume the fluctuations induced on the beam wave by the thin phase screen and the atmospheric turbulence can be considered as independent random processes. This assumption implies that the MCF of the beam in the presence of the atmosphere can be written as

$$\Gamma_{d,a}(\mathbf{r}_1, \mathbf{r}_2, L) = \Gamma_d\left(\mathbf{r}_1, \mathbf{r}_2, L\right)\Gamma_a\left(\mathbf{r}_1, \mathbf{r}_2, L\right), \tag{39}$$

where the first factor is defined by (18) and the second factor is the MCF due to the atmosphere alone, i.e., in absence of the diffuser (or in the limiting case of a weak phase screen, $l_c \to \infty$). Hence,

$$\Gamma_a\left(\mathbf{r}_1, \mathbf{r}_2, L\right) = exp\left[\sigma_a^2\left(\mathbf{r}_1, L\right) + \sigma_a^2\left(\mathbf{r}_2, L\right)\right]exp\left[-T_a\right]exp\left[-\frac{1}{2}\Delta_a\left(\mathbf{r}_1, \mathbf{r}_2, L\right)\right], \tag{40}$$

with (based on a Kolmogorov power-law spectrum)

$$\sigma_a^2\left(\mathbf{r}, L\right) \cong 1.105\,\sigma_1^2\,\Lambda_1^{5/6}\,\frac{r^2}{W_1^2}, \quad r < W_1 \tag{41}$$

$$T_a = 1.33\sigma_1^2\Lambda^{5/6} \tag{42}$$

where σ_1^2 is the Rytov variance and (neglecting an unimportant phase factor)

$$Re\left[\Delta_a\left(\mathbf{r}_1, \mathbf{r}_2, L\right)\right] = \left(\frac{\rho}{\rho_0}\right)^{5/3} \tag{43}$$

where the spatial coherence radius of the Gaussian beam wave [12] is

$$\rho_0 = \left[\frac{8}{3\left(a + 0.618\,\Lambda_1^{11/6}\right)}\right]^{3/5} \left(1.46\,C_n^2 k^2 L\right)^{-3/5}, \qquad a = \begin{cases} \dfrac{1-\Theta_1^{8/3}}{1-\Theta_1}, \Theta_1 \geq 0 \\ \dfrac{1+|\Theta_1|^{8/3}}{1-\Theta_1}, \Theta_1 < 0 \end{cases} \tag{44}$$

where C_n^2 ($m^{-2/3}$) is the refractive index structure parameter. By (41) – (43) combined with (18), (23), the MCF at the detector takes the form

$$\Gamma_{d,a}(\mathbf{r}_1, \mathbf{r}_2, L) = \Gamma_0(\mathbf{r}_1, \mathbf{r}_2, L) exp\left[\left(\frac{2\,\Lambda_1^2}{l_c\left(1 + 4\,q_c\,\Lambda_1\right)} + \frac{1.105\,\sigma_1^2\,\Lambda^{5/6}}{W_1^2}\right)\left(r_1^2 + r_2^2\right)\right]$$

$$\times exp\left[-\left(4\,q_c\,\Lambda_1 + 1.33\,\sigma_1^2\,\Lambda_1^{5/6}\right)\right] exp\left[-\left(\frac{\left(\Theta_1^2 + \Lambda_1^2\right)\rho^2}{\left(1 + 4\,q_c\,\Lambda_1\right)l_c^2}\right) + \left(\frac{\rho}{\rho_0}\right)^{5/3}\right] \tag{45}$$

The size of the beam in this case can be deduced from (45) and approximated by:

$$W_{1,d,a} = W_1\left(1 + 4\,q_c\,\Lambda_1 + 1.33\,\sigma_1^2\,\Lambda_1^{5/6}\right)^{1/2} \tag{46}$$

The last expression is similar to the corresponding result in [4], but differs due to the approximation of the atmospheric spectrum by a Gaussian in [4] as commonly used in classic literature.

In Figure 4 we plot the effective beam size $W_{1,d,a}$ scaled by the initial beam radius W_0 versus the correlation length l_c (solid curve). For a comparison the corresponding result based on the model [4] is plotted as well (dotted curve). For both curves $W_0 = 2.5\,cm$, $\lambda = 0.5\,\mu m$, $L = 500\,m$, $\sigma_1^2 = 0.98$. For values $l_c > 0.01$ the difference between Kolmogorov spectrum model and its Gaussian approximation used in [4] result in the significant deviation of the approximated beam size. This difference saturates at $l_c \approx 0.06 – 0.07$. Therefore for the moderate and weak diffuser ($l_c > 0.01$) the Gaussian model underestimates the effective beam size and consequently the power loss in the receiver (with error ≈*12%*).

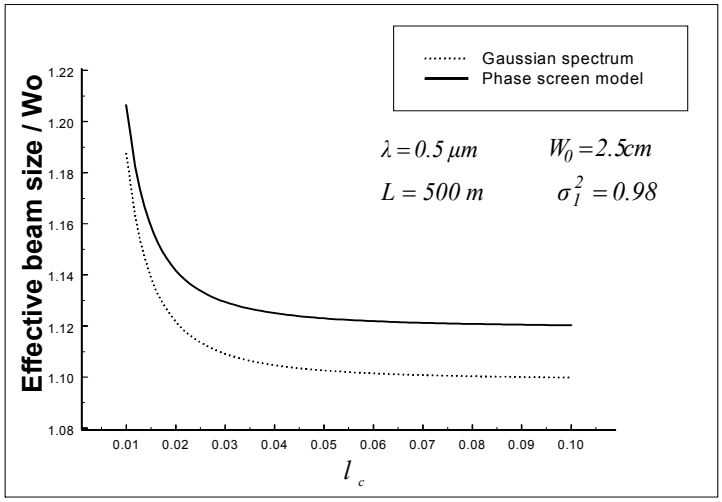

Figure 4. Effective beam size in the atmosphere.

The average speckle size is derived from the last exponential factor in (45) with approximation $\left(\frac{\rho}{\rho_0}\right)^{5/3} \approx \left(\frac{\rho}{\rho_0}\right)^2$, i.e.

$$\rho_{1,d,a} = \left(\frac{\Lambda_1^2 + \Theta_1^2}{l_c^2 \left(1 + 4\, q_c \Lambda_1\right)} + \frac{1}{\rho_0^2} \right)^{-\frac{1}{2}} \tag{47}$$

or, equivalently, in terms of the effective beam size (20)

$$\rho_{1,d,a} = \frac{l_c W_{1,d}}{W_0} \left(1 + \frac{W_{1,d} l_c^2}{W_0 \rho_0^2} \right)^{-1/2} \tag{48}$$

where the first factor is induced by the diffuser alone [see (23)], and the second is the perturbation due to the atmosphere.

Figure 5 shows the effective average speckle size (defined in (47)) as a function of q_c in weak atmospheric turbulence (solid curve). $W_0 = 2.5\,cm$, $\lambda = 0.5\,\mu m$, $L = 500\,m$, $C_n^2 = 10^{-14}\ m^{-2/3}$. The corresponding result derived in [5] is shown for comparison (dotted curve).

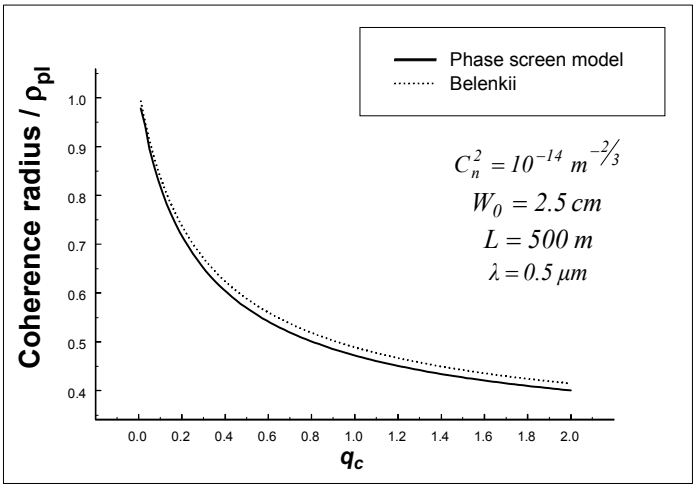

Figure 5. Coherence radius scaled by coherence radius of plane wave vs. q_c.

The mean irradiance of the beam is similarly deduced from MCF (44) for $\mathbf{r}_1 = \mathbf{r}_2 = \mathbf{r}$

$$\left\langle I_{1,d,a}(\mathbf{r}, L) \right\rangle = \left\langle I_{1,d}(\mathbf{r}, L) \right\rangle exp\left(\frac{2.21 \sigma_1^2 \Lambda^{5/6}}{W_1^2} \right), \tag{49}$$

where $\left\langle I_{1,d}(\mathbf{r}, L) \right\rangle$ is defined in (21).

The variance of the angle of arrival fluctuations in the presence of the atmosphere can be approximated by

$$\sigma_{\beta,d,a}^2 \cong \frac{1}{k^2} \left[\frac{2\left(\Lambda_1^2 + \Theta_1^2\right)}{\left(1 + 4\, q_c \Lambda_1\right) l_c^2} + \rho_0^{-5/3} \right] = \left[\frac{2 W_0^2}{k^2 W_{1,d}^2 l_c^2} + 0.55\, C_n^2 L \right] \tag{50}$$

4.2. Scintillation Index.

The effect of the diffuser on the scintillation index in weak atmospheric turbulence is analyzed here for a case of a slow detector only. Generally, there is a correlation between perturbations induced by the diffuser and atmosphere, however for a slow detector the diffuser-induced part of scintillation is negligible as well as its correlation with atmosphere. Therefore the only term representing the (on-axis) scintillation index is [12]

$$\sigma_a^2(L,0) = 8\pi^2 k^2 L \int_0^1 \int_0^\infty \kappa \Phi_n(\kappa) exp\left(-\frac{\Lambda_e L\kappa^2 \xi}{k}\right)\left[1 - cos\left(\frac{L\kappa^2}{k}\xi\left(1-\overline{\Theta}_e\xi\right)\right)\right] d\kappa d\xi \tag{51}$$

For the Kolmogorov spectrum, $\sigma_a^2(L,0)$ can be approximated [12] by

$$\sigma_a^2(L,0) \cong 3.86\,\sigma_1^2 \left\{0.40\left[(1+2\Theta_e)^2 + 4\Lambda_e^2\right]^{5/12} cos\left[\frac{5}{6}tan^{-1}\left(\frac{1+2\Theta_e}{2\Lambda_e}\right)\right] - \frac{11}{16}\Lambda_e^{5/6}\right\} \tag{52}$$

Parameters Λ_e and Θ_e in (51) and (52), however, should differ from Λ_1 and Θ_1 defined by (6) due to the fact that the beam, passing through the diffuser acquires new properties. The diffuser acts as a collection of independent scattering cells of size on the order of l_c which changes the size of the beam (see (20)) and its phase front radius of curvature with propagation distance. The "effective" focal length imposed on the beam by the cumulative action of independent cells can be deduced from the phase component of the free-space MCF (18), i.e.

$$\frac{1}{F_e} = -\frac{1}{L}\left(1 - \frac{\Theta_1}{1+4\Lambda_1 q_c}\right) \tag{53}$$

The focal length F_e varies between $-L$ for a strong diffuser and positive infinity for a weak diffuser. Using characteristics F_e in (53) and $W_{1,d}$ in (20) of the beam destroyed by the diffuser we define effective pupil plane parameters

$$\Lambda_e = \frac{2L}{kW_e^2} = \frac{\Lambda_1}{1+4\Lambda_1 q_c}, \qquad \Theta_e = 1 + \frac{L}{F_e} = \frac{\Theta_1}{1+4\Lambda_1 q_c} \tag{54}$$

For a case of a strong diffuser effective parameters approach zero and the beam acquires properties of spherical wave after short propagation distance, while in the absence of the diffuser Λ_e and Θ_e coincide with Λ_1 and Θ_1 respectively.

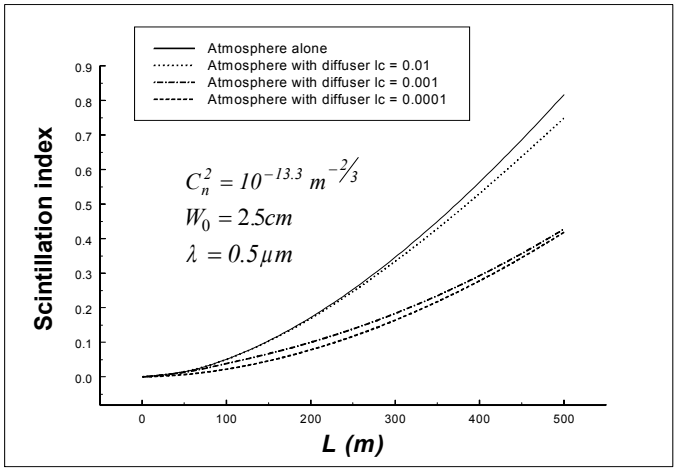

Figure 6. The effect of the diffuser on the scintillation index in the atmospheric turbulence vs. the propagation distance L.

In Figure 6 we compare the scintillation index of the Gaussian beam propagated through the atmosphere in the absence of the diffuser (solid curve) with that given by (53) for different values of the correlation length versus the propagation distance L. Input parameters are $W_0 = 2.5\,cm$ and $\lambda = 0.5\,\mu m$, $C_n^2 = 10^{-13.3} m^{-2/3}$. For smaller values of l_c the scintillation can be considerably reduced. However, the effect saturates for l_c on the order of 10^{-3} and can be considered as optimal competing with power loss in the system.

In the case of a fast detector and strong/moderate diffuser the scintillation index of the detector in vacuum (Figure 3) has to be taken into account as well as its correlation with atmosphere.

5. CONCLUDING REMARKS.

The complex phase screen model introduced in [11] was adjusted to the one-way propagation of the partially coherent Gaussian beam. Partial coherence of the wave (caused by the diffuser with Gaussian spectrum model) is modeled by a focusing effect discussed in Section 2. For the case of free space propagation of the MCF the model reproduces classic results. The effective mutual coherence function (and consequently, the size of the beam, the intensity, the correlation length and the angle of arrival fluctuations) was derived in the pupil plane and in the image plane of the receiver. Beam size, correlation length and the mean irradiance are the same as in [4]. However, in the presence of the atmospheric turbulence our results are slightly different (for example, see Figure 4.) due to the fact that the model under study based all calculations of atmospheric effects on the Kolmogorov spectrum model. The result for coherence radius is in good agreement with [5].

The effect of the diffuser on scintillation was investigated as well. For the case of a fast detector the scintillation index was derived for the free space propagation as well as in weak atmospheric turbulence. In the limit of a strong diffuser our model predicts scintillation on the order of unity in agreement with [7]. The effect of the diffuser on the scintillation index in the presence of atmosphere for a slow detector case is in agreement with [1]. Possibility to control the scintillation by "tuning" the strength of the diffuser is shown in Figure 6.

Effective beam parameters due to the diffuser were introduced in (53). They appear from the second order free space MCF and can be used for fourth order statistics (scintillation index) in the atmosphere.

The main advantage of this phase screen model stems from its flexibility about various atmospheric spectrums and more complex optical systems.

One important case of the scintillation index for a fast detector in atmospheric turbulence is yet to be investigated. High data rates together with controllable level of scintillation would have advantage for lasercom systems. Also, the model for partially coherent beam can be extended to the strong atmospheric turbulence (similarly to the coherent beam case in [13]).

6. REFERENCES.

1. V. A. Banakh, V.M. Buldakov, V. L. Mironov, "Intensity fluctuations of a partially coherent light beam in a turbulent atmosphere", *Opt. Spectrosk*., 54, 1054-1059 (1983).
2. L. Mandel, E.Wolf, *Optical Coherence and Quantum Optics* (Cambridge University Press, Cambridge, 1995)
3. J. W. Goodman, *Statistical optics*, (John Wiley & Sons, 1985)
4. J. C. Ricklin, F. M. Davidson, *Atmospheric turbulence effects on a partially coherent Gaussian beam: Implications for free space laser communication*, (JOSA A, to appear).
5. M. S. Belenkii, A.I. Kon, V.L. Mironov, *Turbulent distortions of the spatial coherence of a laser beam*, Kvantovaya Electron. (Moscow), **4**, 517-523 (1977).
6. A. C. Schell, *The multiple Plate Antenna* (Doctoral Dissertation, Massachusetts Institute of Technology, Cambridge, Massachusetts, 1961).
7. Y. Baykal, M. A. Plonus, S. J. Wang "The scintillations for a weak atmospheric turbulence using a spatially partially coherent source", Radio science, Vol.18, **4**, 551-556 (1983).
8. J. C. Leader, "Intensity fluctuations resulting from a spatially partially coherent light propagating through atmospheric turbulence", J. Opt. Soc. Am. A, Vol.69, **1**, 73 – 84 (1979)
9. Y. Baykal, M. A. Plonus, "Intensity fluctuations due to a spatially partially coherent source in atmospheric turbulence as predicted by Rytov's method", J. Opt. Soc. Am. A, Vol.2, **12**, 2124 – 2132 (1985).

10. L. Fante "Intensity fluctuations of an optical wave in a turbulent medium, effect of source coherence", Opt. Acta, **28,** 1203-1207 (1981).
11. O. Korotkova, L.C. Andrews "Speckle propagation through atmospheric turbulence: effects of partial coherence of the target", (SPIE pr., 2002)
12. L. C. Andrews, R. C. Phillips *Laser beam propagation through random media* (SPIE Opt. Eng. Press, Bellingham, 1998)
13. L. C. Andrews, R. C. Phillips, C. Y. Hopen *Laser beam scintillation with applications* (SPIE Opt. Eng. Press, Bellingham, 2001)

* olga_korotkova@hotmail.com; ** landrews@pegasus.cc.ucf.edu; *** phillips@mail.ucf.edu